Polymer Chemistry

Accepted Manuscript

ROYAL SOCIETY OF CHEMISTRY

www.rsc.org/polymers

Hypersulfonated Polyelectrolytes: Preparation, Stability and Conductivity

Cite this: DOI: 10.1039/x0xx00000x

Shogo Takamuku,[a,b,*] Andreas Wohlfarth,[c] Angelika Manhart,[b] Petra Räder[b] and Patric Jannasch[a,**]

Received 00th January 2012,
Accepted 00th January 2012

DOI: 10.1039/x0xx00000x

www.rsc.org/

Specially tailored polyelectrolytes are becoming important as energy-related materials. Here we explore a synthetic strategy to prepare fully aromatic polymers containing single phenylene rings in the backbone functionalized with four sulfonic acid groups. Thioether bridges of semifluorinated poly(arylene thioether)s were oxidized to sulfone bridges, followed by substitution of all fluorines by NaSH and quantitative oxidation of the resulting thiol groups. This gave poly(arylene sulfone)s containing octasulfonated biphenyl units, reaching ion exchange capacities up to 8 meq. g^{-1} and unprecedented high local sulfonic acid concentrations. These polyelectrolytes are stable up to 300 °C under air and achieve proton conductivities of up to 90 mS cm^{-1} at 120 °C and 50% relative humidity. Despite the excellent performance of this unique new class of hypersulfonated polymers, our data suggests that incomplete proton dissociation may ultimately limit the conductivity of highly sulfonated polymers.

Introduction

One of the central challenges in materials research is to develop synthetic strategies for new materials and to explore the limits of their properties. A good example relates to polymers functionalized with sulfonate groups where synthetic methods and properties have been significantly studied and advanced over the last decade.[1-4] In the form of thin films, these materials are becoming increasingly important for membrane processes such as reverse osmosis for production of drinking water[3] and devices such as electrolyzers for gasification,[4] lithium polymer[5] and vanadium redox flow batteries for energy storage,[2] and fuel cells for energy conversion.[1] The key material requirements are efficient and selective transport properties for water and ions, in combination with high chemical and thermal stability.[6] One of the most promising synthetic strategies to emerge from the vast number of studies published up until now is to utilize fully aromatic polymers with a controlled density and distribution of the sulfonate groups along the polymer chain.[6,7,8] In this context, it has remained a special challenge to prepare fully aromatic polymers containing very high concentrations of sulfonate groups attached to specific phenylene rings in the structure.[9-13] These polyelectrolytes thus have a high concentration of charge carriers (counter ions) to facilitate, *e.g.*, the proton conductivity of fuel cell membranes at low water contents (low relative humidity [RH]).[1,6]

In general, sulfonations involving common agents such as sulfuric and chlorosulfonic acid are directed to electron-rich phenyl rings in aromatic polymers such as poly(ether sulfone)s and poly(ether ether ketone)s.[14] These positions are activated for electrophilic substitution reactions through the ease of formation of the intermediate σ-complex. Concurrently, this also means that the sulfonic acid groups become activated for hydrolysis at high water activities and elevated temperature because the formation of the σ-complex also initiates desulfonation reactions.[15] By employing harsher conditions (*e.g.*, fuming sulfuric acid at elevated temperature) it is possible to also sulfonate deactivated electron-poor rings, but this irrevocably causes severe side reactions which lead to very poor material properties.[16] Moreover, after attaching the first sulfonate group the phenyl ring becomes highly deactivated for further sulfonation. Thus it remains an important challenge to develop efficient synthetic methodologies to place one or more sulfonic acid groups on aromatic rings to promote, *e.g.*, proton conductivity at low water contents without sacrificing stability. Previously Kreuer *et al.* have prepared a poly(phenylene sulfone) (designated S220) where each phenylene ring of the backbone was mono-sulfonated and exclusively connected by electron-withdrawing sulfone linkages.[10] S220 thus had an ion exchange capacity (IEC = mmol SO_3H per g dry membrane) of 4.5 meq. g^{-1} and excellent thermooxidative and hydrothermal stability in combination with a proton conductivity exceeding σ = 0.1 S cm^{-1} at RH = 50%, 120 °C. Very recently, Litt *et al.* prepared a poly(*p*-phenylene) where each phenylene ring in the chain carried two sulfonic acid groups by employing an Ullmann coupling of disulfonated 1,4-dibromobenzene and 4,4'-dibromobiphenyl.[17,18] To our knowledge, this exceptional polyelectrolyte has the highest IEC (7.5 meq. g^{-1}) of any sulfonated aromatic polymer reported so far, and showed a proton conductivity of 0.1 S cm^{-1} (RH = 30%, T = 120 °C).

In the present work, we set out to explore the advantages and limitations of highly sulfonated aromatic copolymers, and have only given a few brief implication of the application in electrochemical cells. Thus we have pushed the limit to the extreme by utilizing a new methodology to covalently attach four sulfonic acid groups to single phenylene rings in the main chains of aromatic polymers.[19] A key to success was to move away from traditional sulfonation procedures and the use of, *e.g.*, sulfuric acid or chlorosulfonic acid. This would have caused severe polymer degradation through chain-breaking reactions,[15] crosslinking and intramolecular cyclizations under the very harsh conditions necessary to reach the exceptionally high levels of functionalization.[12,20,21] To form the C-S bonds we instead utilized an efficient substitution reaction in which the highly activated fluorine atoms of perfluoroaryl sulfone units are displaced by the strongly nucleophilic thiolate anion. Here it was imperative to carefully select aromatic polymer backbones which are insensitive to nucleophilic attack under the conditions employed, *i.e.*, to avoid transetherication reactions.[22,23] Subsequently, the aromatic thiol groups are quantitatively oxidized to form the sulfonic acid groups. Because of their exceptionally high local concentration of

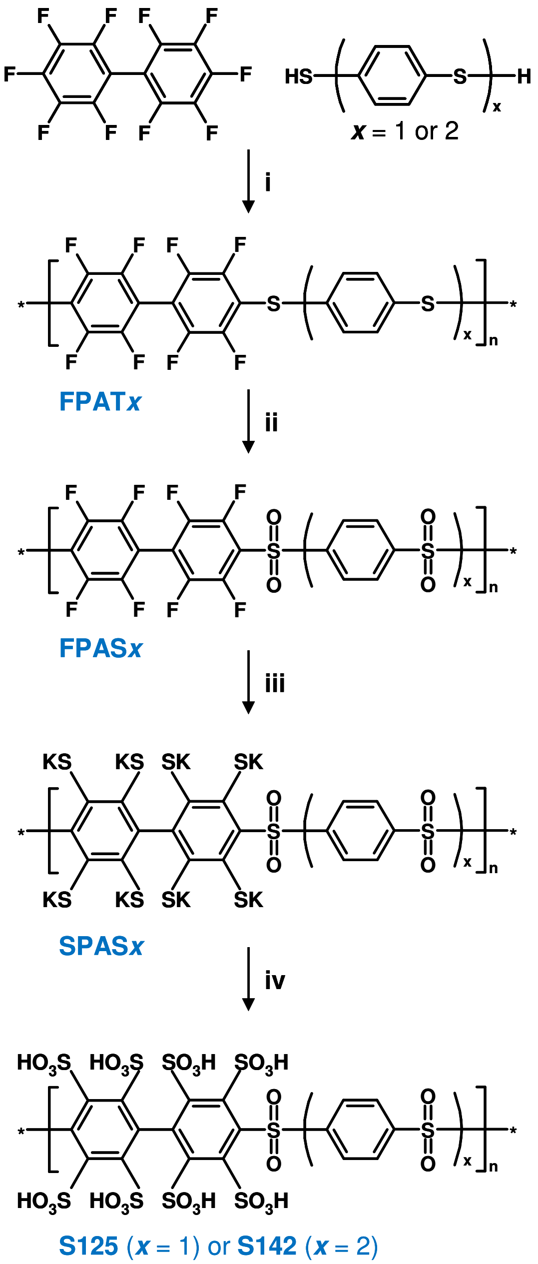

Scheme 1. Synthetic route to the hypersulfonated aromatic polymers S125 and S142: (i) K_2CO_3, 80 °C, 17 h; (ii) H_2O_2, H_2SO_4, AcOH, 30 °C, 48 h; (iii-1) NaSH, K_2CO_3, NMP, toluene, 160 °C, 4 h; (iii-2) NaSH, K_2CO_3, NMP, 205 °C, 20 h; (iv-1) H_2O_2, H_2O, 40 °C, 24 h; (iv-2) ion-exchange resin to H^+.

sulfonic acid groups, we designate these new polyelectrolyte materials as hypersulfonated polymers.

Results and Discussion

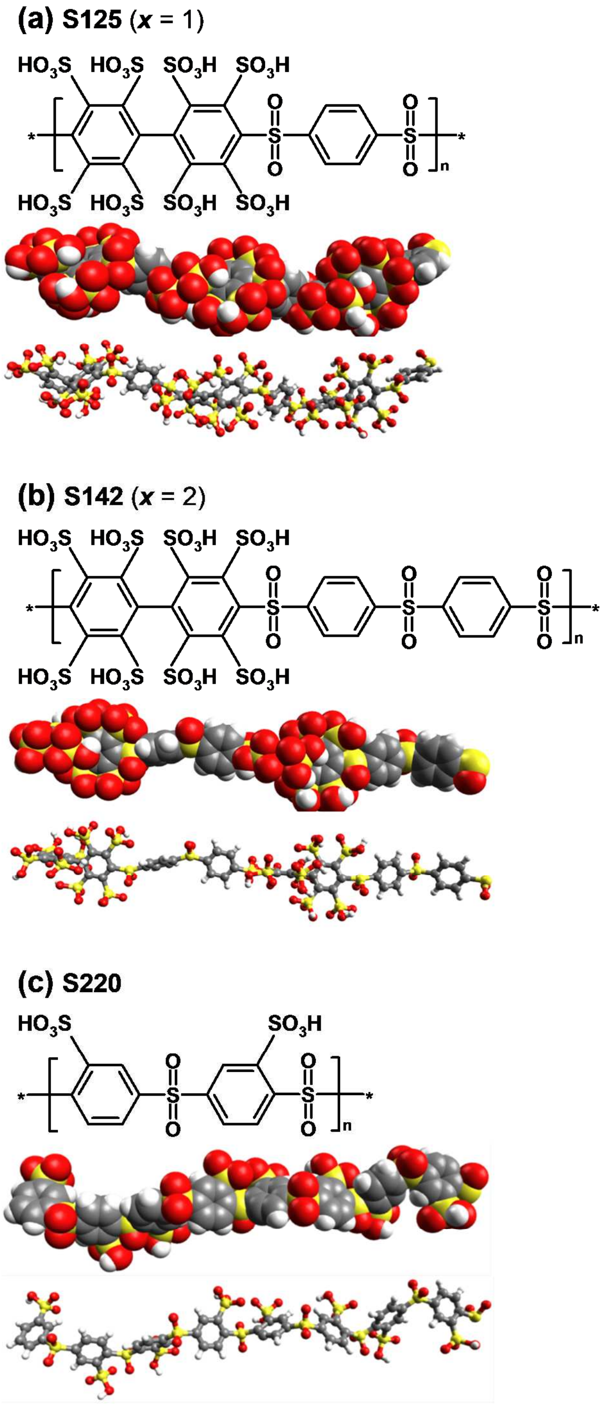

Scheme 2. Structure and space-filling models of two repeating units of S125 (a), S142 (b)and S220 (c), respectively.

We prepared two fully aromatic poly(arylene sulfone)s with octasulfonated biphenyl units in the repeating unit. First, two semifluorinated poly(arylene thioether)s (FPAT1 and FPAT2) were synthesised in mild K_2CO_3-mediated polycondensations of decafluorobiphenyl (10F) and either 1,4-benzenedithiol (BDT, x = 1) or 4,4'-thiobisbenzenethiol (TBBT, x = 2), as shown in **Scheme 1**. Carefully controlled polymerization conditions were needed to depress branching reactions that potentially arise from the high reactivity and multi-functionality of 10F. ^{19}F and ^{1}H nuclear magnetic resonance (NMR) spectroscopy successfully confirmed the structure of the two polymers with only very small signals originating from 10F units present as chain ends or branching units to indicate a reasonably high molecular weight and degree of linearity (**Fig. 1** and **2**).[24] The two relatively large signals around -150 and -160 ppm in the spectrum of FPAT1 may be explained by the very high reactivity between BDT and 10F (**Fig. 1**). In the next step, the thioether bridges of the polymers were oxidized to

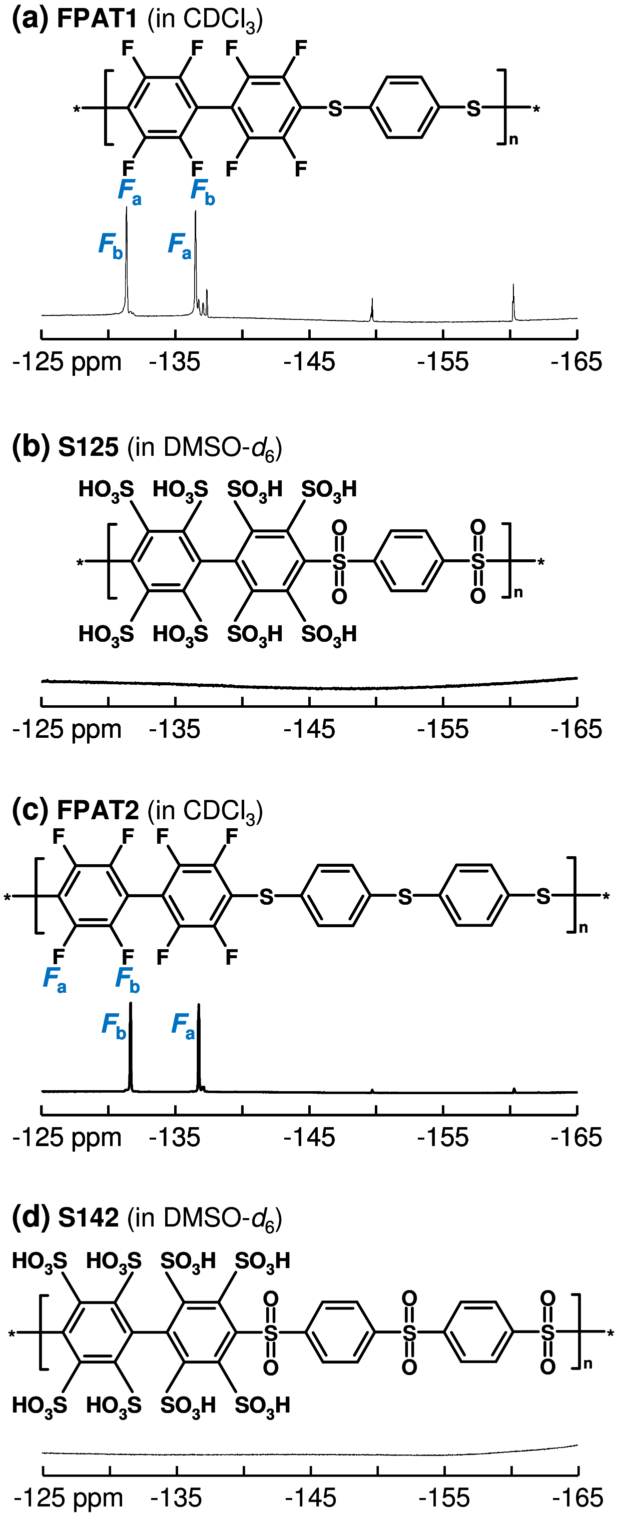

Figure 1. ^{19}F NMR spectra of (a) FPAT1 (in $CDCl_3$), (b) S125 (in DMSO-d_6), (c) FPAT2 (in $CHCl_3$) and (d) S142 (in DMSO-d_6).

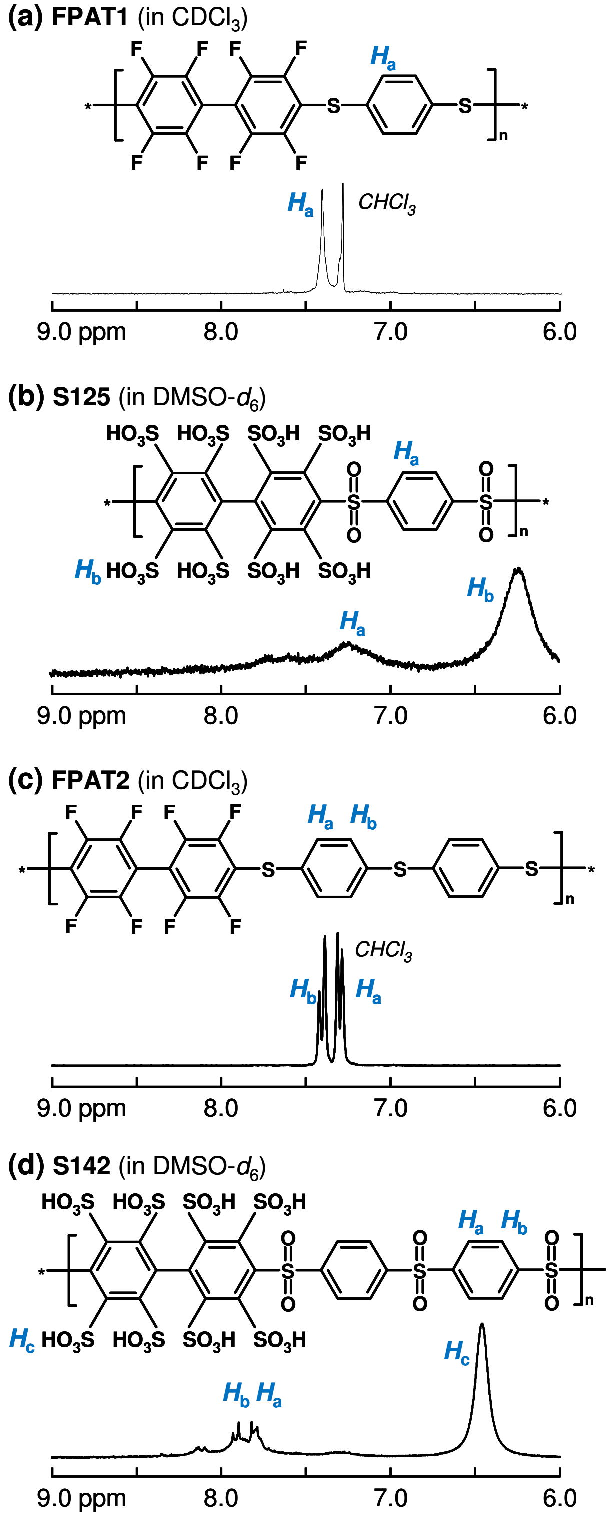

Figure 2. ^{1}H NMR spectra of (a) FPAT1 (in $CDCl_3$), (b) S125 (in DMSO-d_6), (c) FPAT2 (in $CHCl_3$) and (d) S142 (in DMSO-d_6).

sulfone linkages using a mixture of H_2O_2 and H_2SO_4 in AcOH to form the corresponding semifluorinated poly(arylene sulfone)s (FPAS1 and FPAS2, respectively, **Scheme 1**).[9-11] The sulfone linkages were formed to activate the fluorine atoms for the subsequent nucleophilic aromatic substitution. In addition, the polymer backbones were stabilized against transetherifications during the subsequent reaction with the thiolate which may otherwise cause randomization, transformation and chain-scission of the polymer structure.[22,23]

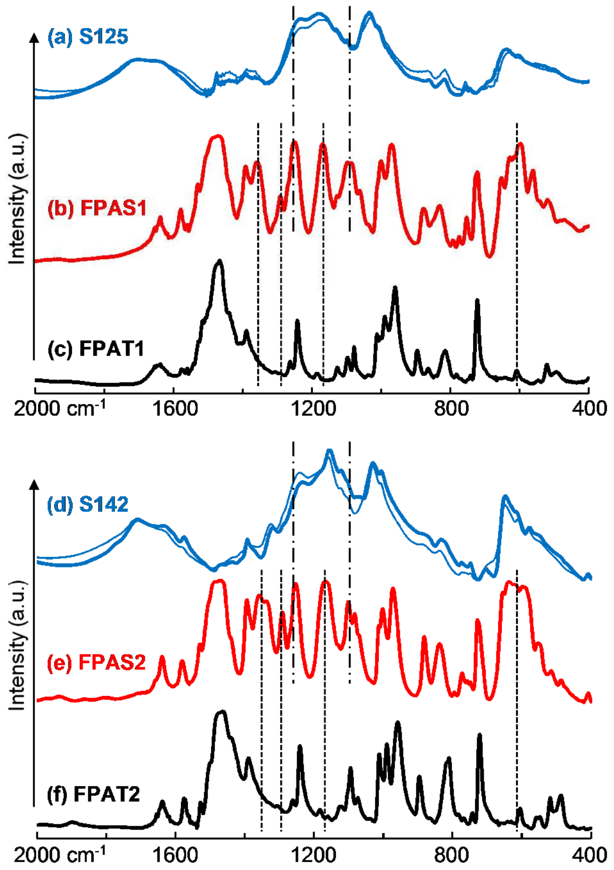

Figure 3. FTIR spectra of (a) S125 and (d) S142 (the thin lines are the spectra of the samples exposed at 200 °C for 2 h under air), (b) FPAS1, (c) FPAT1, (e) FPAS2 and (f) FPAT2. The dash lines included in the graphs are guide to the eye.

Both poly(arylene sulfone)s were completely insoluble in common solvents which prevented NMR analysis. Instead, FTIR spectra were collected to qualitatively verify the success for the oxidation. As seen in **Fig. 3b** and **3e**, three new peaks clearly appeared at 1400-1150 cm^{-1}, due to the stretching of the SO_2 groups. In addition, the band arising from SO_2 scissor deformation at 600 cm^{-1} also indicated the successful oxidation.[25]

The activated fluorine atoms of the poly(arylene sulfone)s were substituted in a thiolation reaction using a 50% excess of NaSH in *N*-methyl-2-pyrrolidinone (NMP) containing K_2CO_3 at 205 °C during 20 h (**Scheme 1**). This reaction was followed by an oxidation of the resulting thiol groups by H_2O_2 to form the sulfonic acid groups.[26] The reaction conditions employed resulted in total displacement, and thus no residual fluorine atoms were detected by ^{19}F NMR analysis of the sulfonated polymer. Concurrently, a broad characteristic peak attributed to protonated water was observed at 6-6.5 ppm (**Fig. 2b** and **2d**). Weak and broad shifts from the aromatic protons were found between 7.7 and 8.2 ppm for S142, and between 7 and 7.8 ppm for S125. The higher chemical shift of S125 may indicate limitations in the oxidation of the thioether to sulfone links. FTIR spectra showed that the two sharp bands due to aryl-F vibration at 1100 and 1250 cm^{-1} disappeared completely after the substitution reaction (**Fig. 3a** and **3d**).[25] Furthermore, a characteristic broad band appeared at 1500-1800 cm^{-1} because of the presence of sulfonic acid hydrate (aryl-SO_3^- H_3O^+), in addition to a very broad and strong band above 2000 cm^{-1} due to the presence of water (see Supplementary Information, **Fig. S1**).[25] Initially, the influence of the temperature and solvent on the reaction was investigated with or without K_2CO_3 in order to identify the optimum conditions. Most of these reactions gave incomplete substitutions, which was readily observed by ^{19}F NMR spectroscopy by the presence of both original and new signals (see Supplementary Information, **Fig. S2**). However, the optimized reactions produced completely water soluble hypersulfonated poly(arylene sulfone)s with octasulfonated biphenyl units in the main chain with theoretical IECs of 8.02 and 7.04 meq. g^{-1}, respectively. This corresponded to equivalent weights (EW = 1000 × IEC^{-1}) of 125 and 142 g mol^{-1}, respectively, and the samples were thus designated S125 and S142, respectively. We confirmed the successful synthesis by ^{19}F NMR, FTIR and size exclusion chromatography (SEC) measurements. Acid-base titrations of aqueous solutions of carefully dried (T = 120 °C under vacuum, 24 h) samples gave IEC = 7.13 meq. g^{-1} for S142, confirming the successful preparation. However, the same titration of S125 gave a lower value, 6.20 meq. g^{-1}, than its theoretical IEC (**Table 1**). The discrepancy was at least partly due to the exceptional hygroscopic character of S125, which was found to absorb

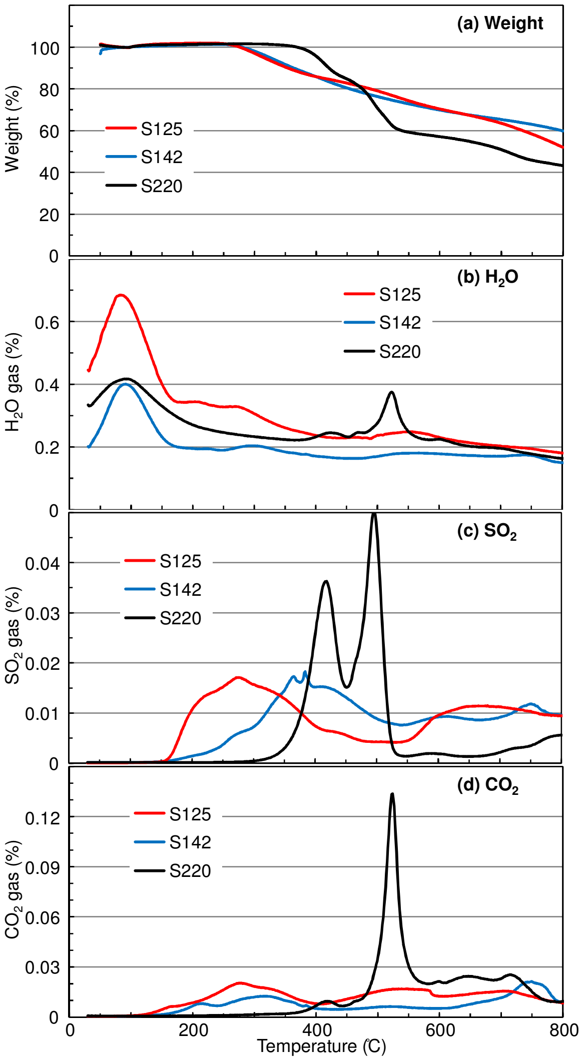

Figure 4. TG-MS data of S125 and S142 in comparison to S220 under nitrogen at 10 °C min^{-1}: (a) Weight loss and evolved (b) H_2O, (c) SO_2, and (d) CO_2 gas.

large amounts of water directly after freeze-drying (Supplementary Information, **Fig. S3**). Moreover, intra- and intermolecular reactions to form anhydrides and cyclic sulfones during heating has previously been reported in hexasulfonated benzenes, and this most probably also occurred in S125 resulting in a reduced concentration of free acid.[27] SEC analysis of the samples in the H^+ form showed a reasonably high molecular weight, and the density was 1.63-1.64 g cm^{-3} for both S125 and S142 (**Table 1**).

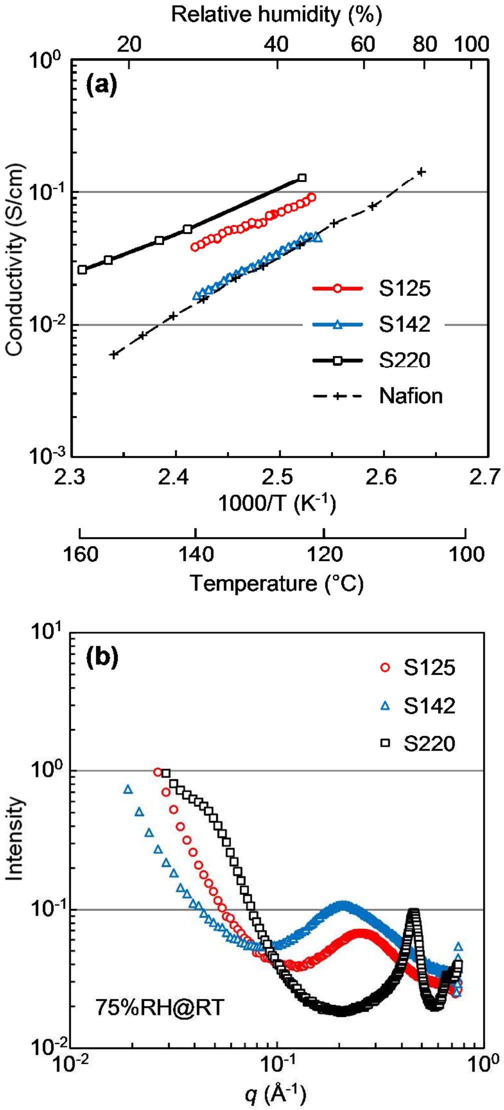

Figure 5. (a) Proton conductivity data of S125 and S142 at constant water pressure (pH_2O = 1 atm). (b) SAXS data of S125 and S142 at 75% RH and room temperature. Data of S220 and Nafion are shown for comparison.

The hypersulfonated polyelectrolytes S125 and S142 have a quite exceptional macromolecular structure and character. Their completely aromatic backbones are devoid of any ether bridges and have exclusively sulfone or direct aryl-aryl bridges which give a very high chain stiffness and thermo-oxidative stability. In addition, the eight sulfonic acid groups on the biphenyl units impose further conformational restrictions. In fact, the adjacent tetrasulfonated rings of the octasulfonated biphenyl units are unable to rotate in relation to each other because of the steric hindrance (**Scheme 2**). The sulfone bridges are strongly electron withdrawing and thus all the aromatic rings are highly electron deficient. This should provide a high hydrolytical stability by strongly impeding the formation of σ-complexes.[9-11,15,28]

FTIR spectra of the hypersulfonated polymers recorded before and after exposure to air at T = 200 °C for 2 h were seemingly identical to indicate high thermal stability (**Fig. 3**). TGA measurements coupled with mass spectroscopy (TG-MS) under N_2 (10 °C min^{-1}) were performed to investigate the degradation behavior in more detail (**Fig. 4**). The thermal decomposition temperature (T_d) at 10 wt.% loss was 353 and 363 °C for S125 and S142, respectively (**Fig. 4a**). Even under air (1 °C min^{-1}), the T_ds were found to be above T = 300 °C, which further indicated high thermal stability (also see Supplementary Information, **Fig. S3**). Careful analysis by mass spectroscopy up to 150 °C showed that only water moisture loosely adsorbed by the hypersulfonated polymers was evolved (**Fig. 4b**). The initial evolution of sulfur dioxide SO_2 (>10 ppm) was observed at T = 163 and 185 °C for S125 and S142, respectively (**Fig. 4c**). This was most probably caused by condensation of adjacent acidic groups releasing the byproduct water moisture as barely seen in **Fig. 4b**. Notably, S125 released significantly more water at T = 100 °C (~0.7% H_2O for S125 and ~0.4% for S142 and S220). The high water adsorption and the early loss of sulfonate groups of S125 was in line with the discrepancy between the theoretical and experimental IEC values, as previously discussed.[27]

The proton conductivity of pressed pellets of S125 and S142 was measured by electrical impedance spectroscopy in the temperature range T = 120-140 °C at a constant absolute water vapor pressure of 1 atm[10] and was compared with that of S220. This corresponds to a RH between approximately 20% and 50% at the respective temperature. As seen in **Fig. 5a**, S142 showed high proton conductivity, reaching σ = 45 mS cm^{-1} at T = 120 °C and RH = 50%. As expected, S125 showed even higher proton conductivity, reaching σ = 90 mS cm^{-1} under the same conditions. However, the conductivity of S125 was still slightly lower than that of S220 (IEC = 4.60 meq. g^{-1}) despite the higher IEC. The data suggests that the very close proximity of the sulfonic acid groups in the hypersulfonated polymers leads to incomplete proton dissociation (counter ion condensation) resulting in a reduced charge carrier concentration, and thus reduced conductivity. Moreover, Paddison et al. recently showed using theoretical considerations that S220 has well distributed hydrophilic domains and well-connected water channels to favor conductivity at low water contents.[29,30] Limited ion dissociation and possible anhydride formation in hypersulfonated systems may potentially alter the distribution of hydrophilic domains leading to a lower connectivity of the water channels in hypersulfonated systems.

The effect of the extremely high local sulfonic acid concentrations on the membrane microstructure was studied by small angle X-ray scattering (SAXS) measurements (**Fig. 5b**). A few features were immediately visible in the scattering pattern of pressed pellets equilibrated at RH = 75% (mol water per mol sulfonate group, λ = 5-7). Pronounced correlation peaks are observed for both S125 and S142 at 0.252 and 0.206 $Å^{-1}$, respectively, corresponding to correlation distances of d = 2.49 and 3.04 nm, respectively. This was similar to the features of S220 (q = 0.460 $Å^{-1}$, d = 1.37 nm). The correlation length d is determined by the most frequently occurring distance between alternating water rich and polymer rich domains. Typically, the polymer domains are expected to become more ordered and narrower with increasing sulfonic

Table 1. Molecular and thermal data of the sulfonated polymers investigated.

	M_n (kDa)	M_w (kDa)	PDI	IEC_{theory} (meq. g^{-1})	$IEC_{titrated}$ (meq. g^{-1})	Density[c] (g cm^{-3})	$T_{d10\%}$[d] (°C)	$T_{d10\%}$[e] (°C)	d[f] (nm)
S125	4.8[a]	10.3	2.12	8.02	6.20[b]	1.64	353	329	2.49
S142	5.7[a]	12.1	2.13	7.04	7.13	1.63	363	311	3.04
S220	20.0[a]	30.0	1.50	4.55	4.60	1.75	420	379	1.37

(a) measured in DMF with LiBr (1 g L^{-1}) at 60 °C; (b) calculated assuming a water content of 29 wt% (see Supplementary Information, **Fig. S3d**); (c) measured with a helium gas pycnometer; (d) measured under nitrogen at 10 °C min^{-1}; (e) measured under air at 1 °C min^{-1}; (f) measured by SAXS at 75% RH and room temperature. $d = 2\pi \times q^{-1}$

acid content,[31,32] but the reverse was observed here. This especially pointed towards an incomplete proton dissociation resulting in less electrostatic interactions to drive the microstructure formation in the hypersulfoned polymers.

In order to explore the limits of our synthetic approach, we made an attempt to prepare a hypersulfonated polymer where all the aromatic positions are substituted with sulfonic acid by preparing a poly(arylene thioether) via polycondensation of 10F and Li_2S (see Supplementary Information, **Scheme S1**). However, we were not able to completely oxidize the thioether bridges of this fully aromatic perfluorinated polymer, possibly because of its high degree of substitution and hydrophobic character. A polyelectrolyte S107 was prepared after substitution and oxidation to form the sulfonic acid groups (**Scheme S1**). However, the low thermal stability of this material prevented further characterization. This clearly showed the limits of our concept when moving to extremely high degrees of sulfonations. All details of S107 are available as Supplementary Information.

Experimental

Synthetic Procedure

The preparation of S125 and S142 is specified below, while a detailed discussion on the preparation of S107 is provoded as Supplementary Information.

Polycondensation: To prepare polymer FPAT2, TBBT (1.499 g, 5.986 mmol, FumaTech), 10F (2.000 g, 5.986 mmol, 99%, Fluorochem) and potassium carbonate (K_2CO_3, 1.241 g, 8.979 mmol, >99.0%, Sigma-Aldrich) were charged to a one-neck 50 mL round-flask with dimethylacetamide (14 mL, 99.5%, Acros) in a Glove box filled with Argon. The polymerization was carried out at 80 °C in a closed system. After 17 h, the viscous solution was poured into deionized water, and the white powder was precipitated out. The product was carefully washed several times using deionized water and 2-propanol (>99.8%, Sigma-Aldrich) via filtration. FPAT2 was dried under vacuum at 30 °C overnight (yield: 3.12 g, 95.7%). In the case of FPAT1, BDT was employed instead of TBBT and polymerized with a gradual increase in reaction temperature from room temperature to 80 °C (yield: >95%).

Oxidation: FPAT2 polymer (3.10 g, 17.1 mmol of Sulfur) was added to a one-neck 250 mL round-flask containing H_2O_2 (14 mL, 166 mmol, 34.5-36.5%, Sigma-Aldrich), H_2SO_4 (15.5 mL, 95-97%, Sigma-Aldrich) and AcOH (62 mL, analytical reagent grade, Fisher Chemical), and the oxidation was completed at 110 °C for 1 h after 48 h at 30 °C. The dispersion was filtered to collect the oxidized powder, and the product FPAS2 was washed several times in deionized water and 2-propanol before it was vacuum-dried at 30 °C overnight (yield: 3.44 g, 94.3%). FPAS1 was prepared using FPAT1 in exactly the same way as for FPAS2 (yield: >90%).

Sulfonation: FPAS2 polymer (2.02 g, 25.23 mmol of Fluorine) was introduced to a one-neck 250 mL round-bottomed flask equipped with Dean-Stark trap, containing 1-methyl-2-pyrrolidinone (50 mL, 99+%, Alfa Aesar), toluene (100 mL), sodium hydrosulfide (NaSH, 4.715 g, ca. 50.46 mmol, >60% purity, Sigma-Aldrich) and K_2CO_3 (34.9 g, 252 mmol). Dehydration was first carried out at 160 °C for 4 h. After removal of toluene, the thiolation was completed by heating at 205 °C for 20 h under Ar. The cooled solution was poured into diethyl ether (>99.8%, Sigma-Aldrich), yielding in a dark brown precipitate. The product was repeatedly washed in fresh diethyl ether, before being transferred to a one-neck 500 mL round-bottomed flask and dissolved in deionized water (220 mL). The oxidation of the thiol groups to sulfonic acid ones was carried out with aq. H_2O_2 (33 mL) during 24 h at 40 °C, followed by 1 h at 110 °C. Next, the solution was filtered and dialyzed (MWCO: 1,000 Da) overnight in deionized water. The product S142 was then ion-exchanged to the H^+ form by passage through an ion-exchange resin (Amberlite®, IR120, H^+ form, Acros), followed by freeze-drying (Vacuubrand RC5 Hybrid Vacuum Pump, set temp. -80 °C, pressure 0.012 mbar, 1 week) in order to obtain the hypersulfonated polymer (yield: 1.46 g, 40.7%). Sample S125 was prepared using the same preparation procedure (yield: ~50%).

Measurement

IR spectroscopy: FTIR spectra were obtained with Perkin Elmer FT-IR System and Spectrum version 5.3.1. software, using KBr pellets containing ca. 1% of measured components prepared by pressing at 10 bar.

NMR spectroscopy: ^1H, ^{13}C and ^{19}F NMR spectra were obtained with Bruker Avance 250 MHz, Bruker Avance DRX 300 MHz and Bruker DSX500 spectrometers at room temperature, using deuterated dimethyl sulfoxide (DMSO-d_6) or chloroform ($CDCl_3$) solutions.

Thermal analysis: TG-MS measurement was performed with Mettler-Toledo TGA/DSC1 (TGA851) coupling with MS Pfeiffer Thermostar, as well as Balzers Quadstar 422 software in nitrogen gas (50 mL min^{-1}) at a heating rate of 10 °C min^{-1} without any preconditioning.

Acid-base titration: IECs of the investigated sulfonated aromatic polymers were analyzed by acid-base titration. The polymers were dried before titration at 85-120 °C in a vacuum oven (Vacuubrand RC5 Hybrid Vacuum Pump, 0.01 mbar) for 3 days. Then, they were dissolved in deionized water and titrated with 0.1 M NaOH using Mettler Titrator DL21.

Chromatography: Molecular weights of polymers were determined by gel permeation chromatography (GPC) in DMF or DMSO solutions with additional LiCl (1 g L^{-1}) at 60 °C or 70 °C, using a Waters 515 system equipped with three consecutive columns (GRAM, 10000, 1000, 100, Polymer Standard Service) calibrated with polystyrene or PMMA (Polymer Standard Service, Germany), equipped with a UV detector (Soma S-3702) and RI detector (ERC 7512, ERMA).

Density measurements: Densities of the dry sulfonated aromatic polymers were obtained with helium-gas pycnometer (Micromeritics AccuPyc 1330) at room temperature. The samples (200-500 mg) were placed in a sample chamber of size 1 cm^3 and dried at 85-120 °C in a vacuum oven (Vacuubrand RC5 Hybrid Vacuum Pump, 0.01 mbar) for 3 days before measurement. From the derived volume and dry weight, the density ρ was calculated according to $\rho = m\ V^{-1}$.

Proton conductivity measurements: The dc conductivities were derived from impedance spectra of a two-electrode arrangement measured by a HP ac impedance analyzer (4192A LF) in the frequency range from 10 Hz to 10 MHz with oscillating voltage of 0.1 V. Conductivity measurements in pure water vapor (pH_2O = 1 atm) were carried out in a double-wall temperature-controlled glass chamber with an open outlet at temperatures between T = 110 and 150 °C. Liquid water was continuously evaporated by a heater and injected into the chamber with a constant flow rate using a digital peristaltic pump (Ismatec). Inside the chamber pressed pellets (P/O/WEBER PW40 hydraulic press, 120 mm cylinder, 20 kN) of polymer powder (diameter 6 mm and total thickness of 2-4 mm) were placed in a porous cylindrical tube with a gold electrode at the bottom. The second gold electrode was pressed from the top onto the pellet by a screw in order to ensure optimum contact. The specific conductivity $\sigma = l\ (A \times R)^{-1}$, where l is the distance between the electrodes, A the area of the pellet, and R the resistance derived from the high-frequency intercept of the complex impedance with the real axis.

X-ray scattering: SAXS measurements were carried out on compressed pellets in the H^+ form (diameter: 6 mm, thickness: 0.2 mm) equilibrated under 75% RH and 25 °C during ~60 h. After equilibration, the samples were quickly placed in sealed sample holders with mylar windows and analyzed at 25 °C. The scattering experiments were performed by using a SAXSess camera (Kratky, Anton Paar) equipped with a CCD detector. CuKa radiation with a wavelength of 0.1542 nm was generated by a PANalytical PW3830 X-ray generator operating at 40 kV and 50 mA.

Conclusions

We have for the first time successfully prepared a new class of hypersulfonated fully aromatic polymers with eight sulfonic acid units attached to each biphenylene unit in the polymer backbone by employing a new sulfonation strategy. This pushes the level of the sulfonic acid functonalization beyond the current state-of-the-art sulfonated polymers and gives access to fully aromatic polyelectrolytes with a hitherto unseen high local sulfonic acid concentration. Although the hypersulfonated polymers possess a high stability and reach very high proton conductivity under low RHs at high temperatures, their performance is still surpassed by S220. Our data suggests that the conductivity of the hypersulfonated polymers was limited by incomplete proton dissociation because of their extremely high local sulfonic acid concentration which also may favour anhydride formation under hot and dry conditions. This ultimately limits the performance of highly sulfonated polymers at low water contents, which will be discussed in detail in a forthcoming publication. We are further investigating the microstructure and physicochemical properties of these polymers, and are also exploring the possibilities of synthesizing hydrophilic-hydrophobic block copolymers based on hypersulfonated precursor blocks in order to prepare robust ion-exchange membranes for use in fuel cells and other electrochemical devices.

Acknowledgements

We thank Christine Rosenauer at MPI-P for the SEC measurements, Marc Obiols-Rabasa and Eva Annika Weiber at Lund University for assistance with SAXS measurements and data treatment, Wolfgang H. Meyer at MPI-P and Klaus-Dieter Kreuer at MPI-FKF for valuable discussions, Klaus Müllen and Katharina Landfester at MPI-P for financial and work environmental support, respectively.

Notes and references

[a] Department of Chemistry, Polymer & Materials Chemistry, Lund University, SE-22 100 Lund, Sweden.
[b] Max Planck Institute for Polymer Research, D-55128 Mainz, Germany.
[c] Max Planck Institute for Solid State Research, D-70569 Stuttgart, Germany.
* Email: shogo.takamuku@solvay.com
** Email: patric.jannasch@chem.lu.se

Electronic Supplementary Information (ESI) available: Further details of the preparation and characterization of the hypersulfonated polymers. See DOI: 10.1039/b000000x/

1 K. D. Kreuer, *Chem. Mater.*, 2014, **26**, 361.
2 X. F. Li, H. M. Zhang, Z. S. Mai, H. Z. Zhang, I. Vankelecom, *Energy Environ. Sci.*, 2011, **4**, 1147.
3 Y. Wibisono, E. R. Cornelissen, A. J. B. Kemperman, W. G. J. van der Meer, K. Nijmeijer, *J. Membr. Sci.*, 2014, **453**, 566.
4 M. Carmo, D. L. Fritz, J. Mergel, D. Stolten, *Int. J. Hydrogen Energ.*, 2013, **38**, 4901.
5 D. T. Hallinan Jr., N. P. Balsara, *Annu. Rev. Mater. Res.*, 2013, **43**, 503.
6 N. W. Li, M. D. Guiver, *Macromolecules*, 2014, **47 (7)**, 2175.
7 T. J. Peckham, S. Holdcroft, *Adv. Mater.*, 2010, **22 (42)**, 4667.
8 Y. Yang, A. Sui, T. J. Peckham, S. Holdcroft, *Adv. Polym. Sci.*, 2008, **215**, 55.
9 G. Titvinidze, K. D. Kreuer, M. Schuster, C. C. de Araujo, J. P. Melchior, W. H. Meyer, *Adv. Funct. Mater.*, 2012, **22**, 4456.
10 M. Schuster, C. C. de Araujo, V. Atanasov, H. T. Andersen, K. D. Kreuer, J. Maier, *Macromolecules*, 2009, **42**, 3129.
11 M. Schuster, K. D. Kreuer, H. T. Andersen, J. Maier, *Macromolecules*, 2007, **40**, 598.

12 S. Takamuku, E. A. Weiber, P. Jannasch, *ChemSusChem*, 2013, **6**, 308.

13 S. Takamuku, P. Jannasch, *Adv. Energy Mater.*, 2012, **2**, 129.

14 K. Matsumoto, T. Nakagawa, T. Higashihara, M. Ueda, *J. Polym. Sci., Part A, Polym. Chem.*, 2009, **47**, 5827.

15 G. Koleva, B. Galabov, J. Kong, H. F. Schaefer, P. V. Schleyer, *J. Am. Chem. Soc.*, 2011, **133**, 19094.

16 C. Iojoiu, M. Marechal, F. Chabert, J. Y. Sanchez, *Fuel Cells*, 2005, **5**, 344.

17 K. Si, R. Wycisk, D. X. Dong, K. Cooper, M. Rodgers, P. Brooker, D. Slattery, M. Litt, *Macromolecules*, 2013, **46**, 422.

18 K. Si, D. Dong, R. Wycisk, M. Litt, *J. Mater. Chem.*, 2012, **22**, 20907.

19 S. Takamuku, P. Jannasch, *SE Pat.*, SE1300225-8 2013.

20 E. Neofotistou, C. D. Malliakas, P. N. Trikalitis, *Chem. Eur. J.* 2009, **15**, 4523.

21 J. P. Bassin, R. J. Cremlyn, J. M. Lynch, F. J. Swinbourne, *Phosphorus, Sulfur Silicon*, 1993, **78**, 55.

22 U. Hoffmann, F. Helmer-Metzmann, M. Klapper, K. Muellen, *Macromolecules*, 1994, **27**, 3515.

23 H. M. Colquhoun, D. F. Lewis, P. Hodge, A. Ben-Haida, D. J. Williams, I. Baxter, *Macromolecules*, 2002, **35**, 6875.

24 X. Yu, A. Roy, S. Dunn, A. S. Badami, J. Yang, A. S. Good, J. E. Mcgrath, *J. Polym. Sci., Part A, Polym. Chem.*, 2009, **47**, 1038.

25 N. B. Colthup, L. H. Daly, S. E. Wiberley, *Introduction to Infrared and Raman Spectroscopy, 3rd edition*, 1990, 261-386.

26 V. Atanasov, M. Burger, S. Lyonnard, L. Porcar, J. Kerres, *Solid State Ionics*, 2013, **252**, 75.

27 E. M. Garanin, Y. V. Tolmachev, R. R. Hoover, S. Adas, S. D. Bunge, M. Gangoda, A. K. Khitrin, S. M. Woods, A. Malkovskiy, N. Solak, C. Wesdemiotis, *J. Org. Chem.*, 2010, **75**, 4860.

28 S. Takamuku, P. Jannasch, *Polym. Chem.*, 2012, **3**, 1202.

29 C. Wang, S. J. Paddison, *J. Phys. Chem. A*, 2013, **117**, 650.

30 C. Wang, S. J. Paddison, *Soft Matter*, 2014, **10**, 819.

31 T. Mochizuki, K. Kakinuma, M. Uchida, S. Deki, M. Watanabe, K. Miyatake, *ChemSusChem*, 2014, **7**, 729.

32 C. C. de Araujo, K. D. Kreuer, M. Schuster, G. Portale, H. Mendil-Jakani, G. Gebel, J. Maier, *Phys. Chem. Chem. Phys.*, 2009, **11**, 3305.